ACS APPLIED MATERIALS & INTERFACES

Research Article

www.acsami.org

Combining Ruthenium(II) Complexes with Metal–Organic Frameworks to Realize Effective Two-Photon Absorption for Singlet Oxygen Generation

Wenxiang Zhang,[†,‡] Bin Li,[*,†] Heping Ma,[*,†] Liming Zhang,[†] Yunlong Guan,[†,‡] Yihe Zhang,[†,‡] Xindan Zhang,[†,‡] Pengtao Jing,[†] and Shumei Yue[*,§]

[†]State Key Laboratory of Luminescence and Applications, Changchun Institute of Optics, Fine Mechanics and Physics, Chinese Academy of Sciences, Changchun 130033, P.R. China

[‡]University of Chinese Academy of Sciences, Beijing 100039, P.R. China

[§]College of Chemistry, Changchun Normal University, Changchun 130032, P.R. China

Supporting Information

ABSTRACT: Singlet oxygen ($^1O_2$), as a reactive oxygen species, has garnered serious attention in physical, chemical, and biological studies. In this paper, we designed and synthesized a new type of singlet-oxygen generation system by exchanging cationic ruthenium complexes (RCs) into anionic bio-MOF-1. The resulting bio-MOF-1&RCs can be used as effective photocatalysts for generation of singlet oxygen under both single-photon and two-photon excitation. Especially, the excellent two-photon absorption (TPA) behavior of bio-MOF-1&RCs aroused our interest greatly because their two-photon absorption band lies in the optical window of biological tissue. Here, we measured the ability of bio-MOF-1&RCs to generate $^1O_2$ by irradiation under both 490 and 800 nm wavelength light in DMF. 1,3-Diphenylisobenzofuran (DPBF) and 2′,7′-dichlorofluorescein (DCFH) were used as typical $^1O_2$ traps to detect and evaluate the efficiency of generation of $^1O_2$ under single-photon and two-photon excitation, respectively. Results indicated that bio-MOF-1&$[Ru(phen)_3]^{2+}$ was able to effectively generate $^1O_2$ under both conditions. Our work creates a novel synergistic TPA system with the excellent photophysical properties of RCs and the unique microporous structure benefit of MOFs, which may open a new avenue for creation of a cancer treatment system with both photodynamic therapy and chemotherapy.

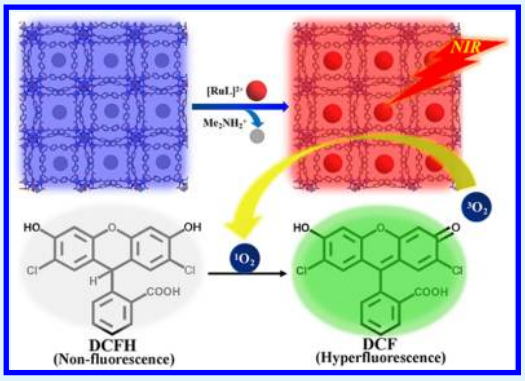

KEYWORDS: *singlet oxygen, photosensitizers, two-photon absorption, ruthenium(II) complexes, metal–organic frameworks*

1. INTRODUCTION

Singlet oxygen ($^1O_2$), a well-known reactive oxygen species (ROS), has garnered serious attention in wastewater treatment, photochemical synthesis, and photodynamic therapy.[1−3] Because directly exciting triplet molecular oxygen ($^3O_2$) to $^1O_2$ is forbidden, a photosensitizer (PS) such as phthalocyanine, methylene blue, porphyrin, etc.[4,5] is necessary to generate singlet oxygen. When the photosensitizer is irradiated with the appropriate wavelength of light, it is promoted from the ground state (S_0) to its first excited singlet state (S_1) and then transformed into the first excited triplet state (T_1) via an intersystem crossing (ISC). The photosensitizer T_1 state can transfer energy to ground-state molecular oxygen ($^3O_2$) nearby to form singlet oxygen[6,7] (Figure S1). However, the absorption bands of most of photosensitizers are mainly in the UV−visible region, which hinders their application in biological tissue.[8,9] A two-photon (TP) excited photosensitizer is one of the most promising materials to expand their absorption window into the long wavelength region.[10,11] Among the different photosensitizers with the TP adsorption capability, polypyridyl ruthenium complexes were found to be excellent candidates owing to their attractive photophysical properties (i.e., high singlet oxygen quantum yield, good light absorption capability, long luminescence lifetime, and excellent chemical stability).[12−14] Indeed, polypyridyl ruthenium complexes have been used in solar energy conversion,[15−17] photocatalysis,[18] sensors,[19] and as therapeutic agents in photodynamic therapy (PDT).[13,20] However, photobleaching, weak resistance to aggregation, and concentration quenching properties of ruthenium complexes limit their $^1O_2$ generation efficiency.[21]

Metal−organic frameworks (MOFs) have aroused widespread research interest because of their intriguing molecular topologies,[22,23] design flexibility,[24] and potential applications in gas storage,[25] separation,[26,27] sensing,[28] and catalysis.[29−32] More recently, MOFs have been designed as an effective light-harvesting active layers in solar cells.[33,34] Because MOFs

Received: May 16, 2016
Accepted: August 2, 2016
Published: August 2, 2016

DOI: 10.1021/acsami.6b05817
ACS Appl. Mater. Interfaces 2016, 8, 21465−21471

can provide highly ordered porous structures, incorporation of PSs in the pore makes them in close proximity to each other but not in direct contact,[35] which can give rise to an efficient platform for energy transfer.[36] Moreover, confinement and isolation of the PSs within the MOF's pore can restrict the aggregation-caused quenching of the PSs,[5,37] providing an attractive platform for a heterogeneous $^1O_2$ generation system.[38,39]

Herein, we present a novel strategy to achieve a TP absorption $^1O_2$ generation system by encapsulating cationic ruthenium complexes (RCs) into the anionic MOF (bio-MOF-1, $[Zn_8(Ad)_4(BPDC)_6O{\cdot}2Me_2NH_2$, 8DMF, $11H_2O]$) through an ion-exchange process.[40,41] The resultant bio-MOF-1&RCs show efficient enhancement of the fluorescence emission by blocking the aggregation of RCs. Moreover, bio-MOF-1&RCs exhibit a remarkable ability to generate $^1O_2$ under both single- and two-photon excitation.

2. RESULTS AND DISCUSSION

RC cations ($[Ru(bpy)_3]^{2+}$, bpy = 2,2′-bipyridine; $[Ru(phen)_3]^{2+}$, phen = 1,10-phenanthroline; and $[Ru(phen)_2hipp]^{2+}$, hipp = 2-(1*H*-imidazo[5,5-*f*][1,10]-phenanthrolin-2-yl)phenol; Figure 1) and bio-MOF-1 were synthesized according to the previously reported method.[42−45] Bio-MOF-1&RCs were prepared through an ion-exchange process (Figure 2 and the Supporting Information). Powder X-ray diffraction (PXRD) was performed to confirm the structure of bio-MOF-1&RCs. As shown in Figure 3, after RC cation exchange, the PXRD spectra of bio-MOF-1&RCs remain unchanged, indicating RC loading does not impact the crystalline integrity of bio-MOF-1. In addition, the stability of the bio-MOF-1&RC structure in water was also measured. As exhibited in Figures S2−4, the PXRD spectra of bio-MOF-1&RCs were constant after the complexes were immersed in water for 10 days, indicating that bio-MOF-1&RCs are stable in water. The content of RCs in the MOF crystals were determined using an inductively coupled plasma-optical emission spectrometer (ICP-OES) (Table S1). It is evident that $[Ru(bpy)_3]^{2+}$, which has a small size, can be easily exchanged into the MOF. By contrast, the Ru content in bio-MOF-1&$[Ru(phen)_2hipp]^{2+}$ was the lowest due to the larger molecular size of $[Ru(phen)_2hipp]^{2+}$.

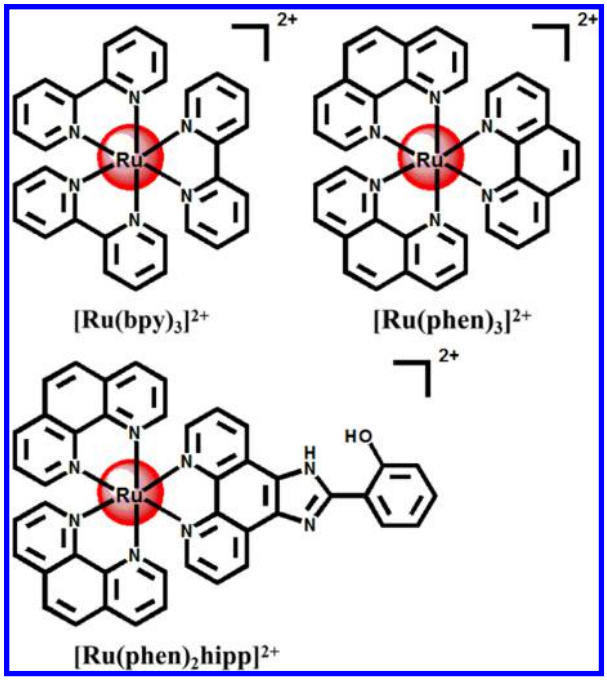

Figure 1. Chemical structures of complexes $[Ru(bpy)_3]^{2+}$, $[Ru(phen)_3]^{2+}$, and $[Ru(phen)_2hipp]^{2+}$.

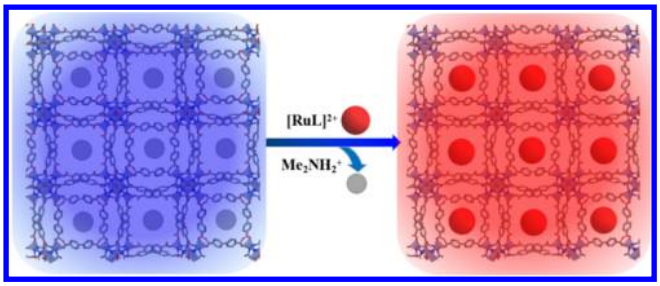

Figure 2. Encapsulation of cationic ruthenium(II) complexes $[RuL]^{2+}$ into the nanospace of bio-MOF-1 (L stands for 2,2′-bipyridine(bpy), 1,10-phenanthroline(phen), or 2-(1*H*-imidazo[5,5-*f*][1,10]-phenanthrolin-2-yl)phenol(hipp)).

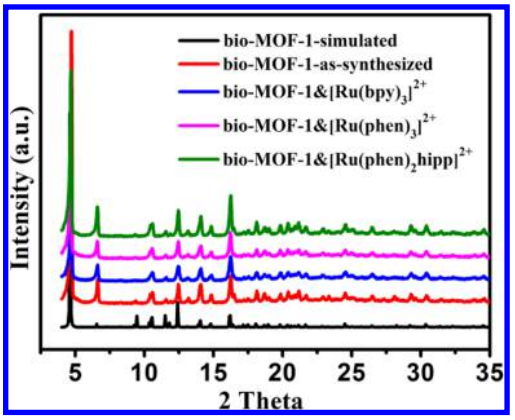

Figure 3. PXRD patterns of bio-MOF-1 and bio-MOF-1&RCs.

Further, we investigated the distribution of RC cations in the bio-MOF-1&RC crystals by confocal scanning microscopy. As shown in Figure 4, the crystals of pure bio-MOF-1 exhibit blue emission derived from the BPDC linkers under ultraviolet light excitation at 330 nm. After RC cations were incorporated into the pore of bio-MOF-1, the bio-MOF-1&RCs display new luminescence emission in the red region. We can clearly see the color of the bio-MOF-1 change from the original blue into orange-red, yellow, and green in the confocal scanning microscopic images. Such significant color changes probably are mainly due to the combination of emissions of bio-MOF-1 (blue) and RCs (red).

The fluorescence emission spectrum of bio-MOF-1 and absorption spectrum of RCs were measured. As shown in Figure S5, RCs have strong absorption ranging from 200 to 550 nm, while the emission spectrum of bio-MOF-1 is between 340 and 500 nm. Obviously, there is spectral overlap between the absorption of RCs and the emission of bio-MOF-1, which suggests that energy transfer from bio-MOF-1 to the RCs can occur within the bio-MOF-1&RCs.

The emission spectra of the $Ru(bpy)_3]^{2+}$ solution, $[Ru(bpy)_3]^{2+}$ powder, and bio-MOF-1&$[Ru(bpy)_3]^{2+}$ were also investigated, and the results are shown in Figure 5a. The $[Ru(bpy)_3]^{2+}$ solution (10^{-4} mol·L^{-1}) and $[Ru(bpy)_3]^{2+}$ powder display relatively weak emission at 613 and 600 nm,

DOI: 10.1021/acsami.6b05817
ACS Appl. Mater. Interfaces 2016, 8, 21465−21471

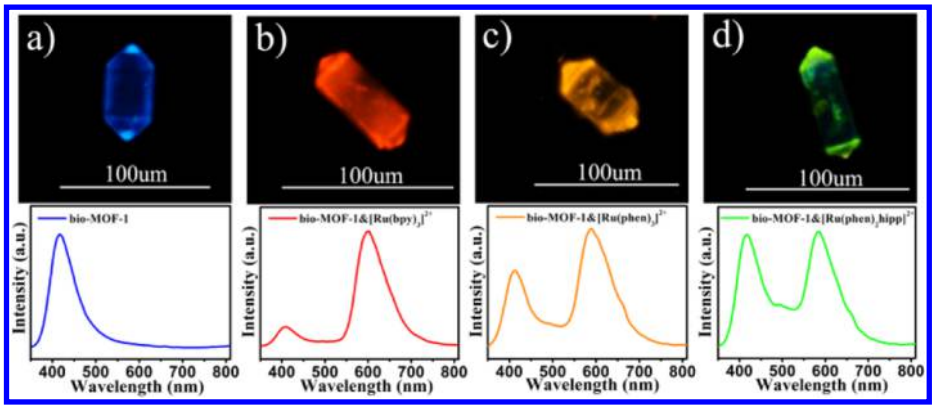

Figure 4. Fluorescence microscopic images and emission spectra of bio-MOF-1&RCs with different RCs of pure bio-MOF-1 (a), bio-MOF-1&$[Ru(bpy)_3]^{2+}$ (b), bio-MOF-1&$[Ru(phen)_3]^{2+}$, (c) and bio-MOF-1&$[Ru(phen)_2hipp]^{2+}$ (d) illuminated with ultraviolet light at 330 nm.

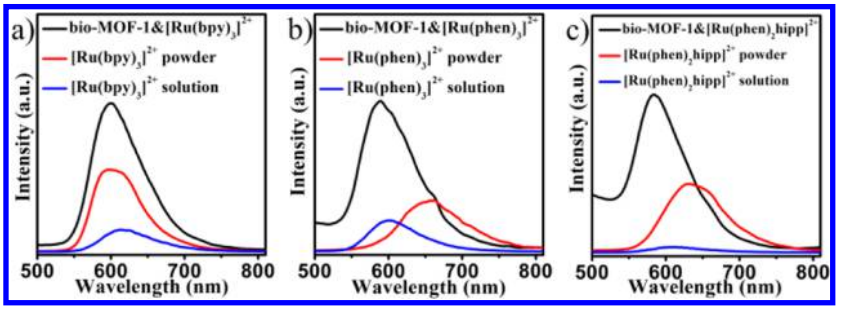

Figure 5. Emission spectra of RCs and bio-MOF-1&RCs excited at 330 nm: (a) $[Ru(bpy)_3]^{2+}$ and bio-MOF-1&$[Ru(bpy)_3]^{2+}$, (b) $[Ru(phen)_3]^{2+}$ and bio-MOF-1&$[Ru(phen)_3]^{2+}$, and (c) $[Ru(phen)_2hipp]^{2+}$ and bio-MOF-1&$[Ru(phen)_2hipp]^{2+}$.

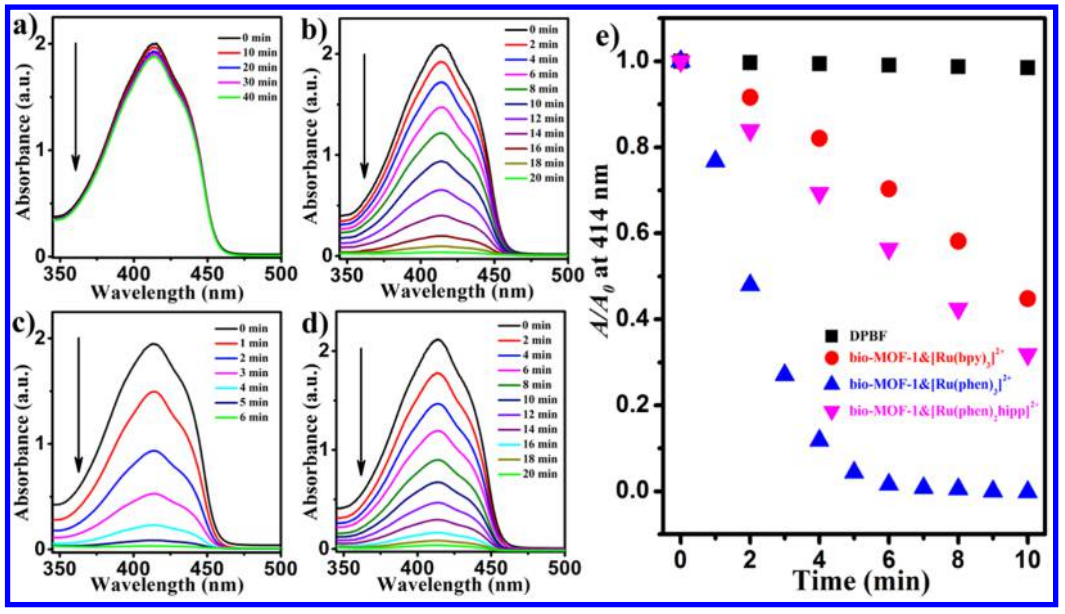

Figure 6. (a) Time-dependent absorption spectra of DPBF (in DMF) upon irradiation at 490 nm without the presence of bio-MOF-1&RCs. Time-dependent absorption spectra of DPBF (in DMF) upon irradiation at 490 nm in the presence of (b) bio-MOF-1&$[Ru(bpy)_3]^{2+}$, (c) bio-MOF-1&$[Ru(phen)_3]^{2+}$, and (d) bio-MOF-1&$[Ru(phen)_2hipp]^{2+}$. (e) Comparison of the decay rate of DPBF alone (black) and in the presence of bio-MOF-1&$[Ru(bpy)_3]^{2+}$ (red), bio-MOF-1&$[Ru(phen)_3]^{2+}$ (blue), and bio-MOF-1&$[Ru(phen)_2hipp]^{2+}$ (purple).

respectively, whereas bio-MOF-1&$[Ru(bpy)_3]^{2+}$ exhibits a much stronger emission at 599 nm. The emission of $[Ru(phen)_3]^{2+}$ and $[Ru(phen)_2hipp]^{2+}$ also show a similar increase in fluorescence intensity in bio-MOF-1 (Figures 5b and c). Such a remarkable emission enhancement can be attributed to the pore confinement of RC molecules within bio-MOF-1. Those RCs molecules, which are confined in the pores of bio-MOF-1, have restricted intramolecular torsional motion and restrained $\pi-\pi$ interactions,[44] which help to markedly diminish the aggregation-caused quenching effect existing in both solution and powder RCs.[46] Moreover, the extended π-conjugation systems in bio-MOF-1 can enhance the light-harvesting ability of bio-MOF-1&RCs,[36] thereby improving the fluorescence emission performance of RCs. In addition, due to

DOI: 10.1021/acsami.6b05817
ACS Appl. Mater. Interfaces 2016, 8, 21465−21471

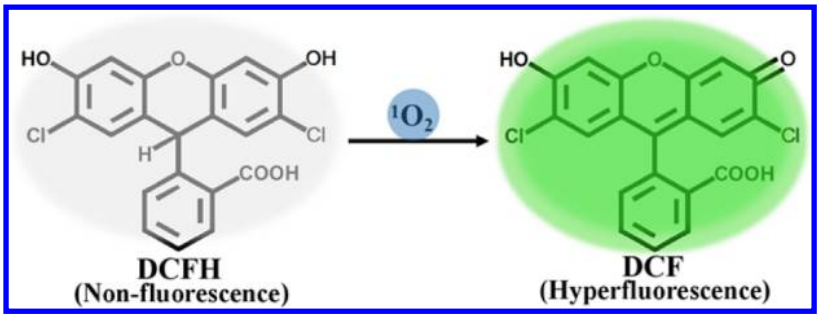

Figure 7. In the presence of generated $^1O_2$, the ROS indicator DCFH is oxidized to release the green fluorophore DCF.

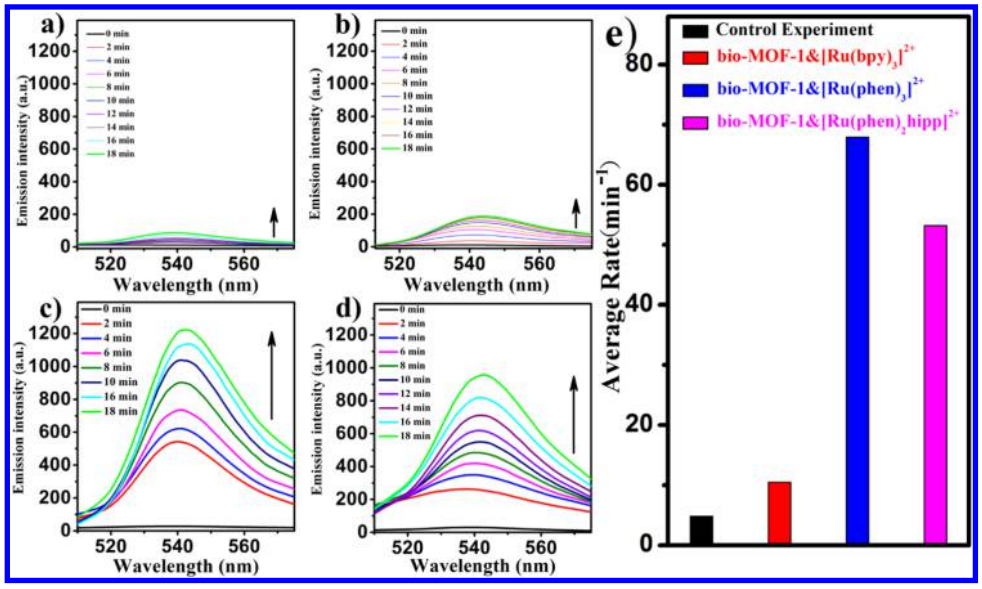

Figure 8. (a) Time-dependent emission spectrum of the fluorescein probe DCF (in DMF, at 540 nm) upon irradiation at 800 nm without the presence of bio-MOF-1&RCs. Time-dependent emission spectra of DCF (in DMF) upon irradiation at 800 nm in the presence of (b) bio-MOF-1&$[Ru(bpy)_3]^{2+}$, (c) bio-MOF-1&$[Ru(phen)_3]^{2+}$, and (d) bio-MOF-1&$[Ru(phen)_2hipp]^{2+}$. (e) Comparison of the average increase rate of DCF in the presence of different bio-MOF-1&RCs within 18 min.

the presence of an intense J-aggregation effect in powder RCs,[47] the emission peak of solid RCs is red shifted compared to that of bio-MOF-1&RCs (Figures 5b and c).

The $^1O_2$ generation efficiency of bio-MOF-1&RCs under single-photon excitation was performed by monitoring the time-dependent absorbance of DPBF at 414 nm. As shown in Figure 6a, in the control experiment without any photosensitizers, the absorbance of DPBF did not change much within 40 min, which revealed that DPBF was stable under the experimental conditions. After addition of bio-MOF-1&$[Ru(bpy)_3]^{2+}$, the characteristic absorption peak of DPBF at 414 nm gradually disappeared within 20 min under 490 nm light irradiation (Figure 6b). When a similar system using bio-MOF-1&$[Ru(phen)_2hipp]^{2+}$ as the photosensitizer was used, DBPF was consumed rapidly, and the absorption of DBPF was completely decayed within 20 min (Figure 6d). Excitingly, the absorption peak of DPBF completely disappeared in only 6 min when bio-MOF-1&$[Ru(phen)_3]^{2+}$ was used in this system, as shown in Figure 6c. Therefore, bio-MOF-1&$[Ru(phen)_3]^{2+}$ possesses the highest efficiency of $^1O_2$ generation among the three composites. Furthermore, the singlet oxygen quantum yields (Φ_Δ) from these bio-MOF-1&RCs, an important parameter for characterization of the efficiency of a triplet PS to produce $^1O_2$ upon photoexcitation, were measured using DPBF as an $^1O_2$ indicator.[3,48] The Φ_Δ values of bio-MOF-1&$[Ru(bpy)_3]^{2+}$, bio-MOF-1&$[Ru(phen)_3]^{2+}$, and bio-MOF-1&$[Ru(phen)_2hipp]^{2+}$ were determined to be 0.86, 0.34, and 0.32, respectively, using $[Ru(bpy)_3]^{2+}$ as the standard (Figure S6), whose Φ_Δ was 0.81 in methanol.[49] The singlet oxygen Φ_Δ of bio-MOF-1&$[Ru(bpy)_3]$ is higher in comparison to those of some photosensitizers such as protoporphyrin IX (Φ_Δ = 0.56), tetraphenylporphyrine (Φ_Δ = 0.63), methylene blue (Φ_Δ = 0.55), rose bengal (Φ_Δ = 0.68),[50] porphyrin derivatives (Φ_Δ = 0.45),[51] and quantum dot photosensitizers (Φ_Δ = 0.43).[52] By contrast, due to the low Ru content of bio-MOF-1&$[Ru(phen)_3]^{2+}$ and bio-MOF-1&$[Ru(phen)_2hipp]^{2+}$, the Φ_Δ values of the two samples are relatively low. However, their Φ_Δ values are still considerably higher compared to those of some newly designed photosensitizers classified to clinical trials such as motexafin lutetium (Φ_Δ = 0.23).[53] A more intuitive contrast of the $^1O_2$ generation efficiency of the three composites is shown in Figure 6e. These results show that bio-MOF-1&RCs can efficiently generate $^1O_2$ via SPA. The bio-MOF-1 could serve as a "cage" to protect the RCs and block the aggregation of RC molecules.[44] Moreover, the porous matrix structure increases the chance of an RC molecule being exposed to molecular oxygen (Figure S7), which is conducive to the energy transfer from the RCs to $^3O_2$.[36,54]

We further studied whether the bio-MOF-1&RCs can generate $^1O_2$ via TPA. For this purpose, we measured the

DOI: 10.1021/acsami.6b05817
ACS Appl. Mater. Interfaces 2016, 8, 21465−21471

two-photon emission spectrum of those bio-MOF-1&RCs under different excitation wavelengths. The excitation wavelength dependent on two-photon emission spectrum of bio-MOF-1&RCs can be seen in Figure S8−10. Obviously, the maximum two-photon excitation wavelengths for bio-MOF-1&RCs are around 800−820 nm. Therefore, we used light with a wavelength at 800 nm as the excitation source to irradiate bio-MOF-1&RCs. Meanwhile, the efficiency of $^1O_2$ generation was evaluated according to the change in the time-dependent fluorescence emission spectrum of the fluorescent probe 2,7-dichlorofluorescein (DCFH). DCFH can be oxidized by singlet oxygen and at the same time rapidly release the green emission DCF (Figure 7),[20] and DCF has a marked emission peak at 540 nm. By monitoring the time-dependent emission intensity change of DCF at 540 nm, we can investigate $^1O_2$ generation efficiency of bio-MOF-1&RCs under TP excitation.[20] As can be seen in Figure 8, the control experiment without addition of bio-MOF-1&RCs exhibited only small spectral changes under the experimental conditions (Figure 8a). In sharp contrast, we can see there is an observable increase in the emission spectrum at 540 nm in the presence of bio-MOF-1&$[Ru(phen)_3]^{2+}$ and bio-MOF-1&$[Ru(phen)_2hipp]^{2+}$ under continuous illumination (Figures 8c and d), which indicates that the photocatalytic activity of bio-MOF-1&$[Ru(phen)_3]^{2+}$ and bio-MOF-1&$[Ru(phen)_2hipp]^{2+}$ are high. While bio-MOF-1&$Ru(bpy)_3]^{2+}$ shows a relatively low photoactivity, which can be reflected through the small change in the emission spectrum at 540 nm (Figure 8b). At the same time, we also noticed that the solution color became green and increased gradually along with illumination time, which also demonstrates that DCFH in solution has been oxidized to DCF. These data suggest that bio-MOF-1&RCs can realize TP excitation in NIR to generation $^1O_2$. The abilities of bio-MOF-1&RCs to generate $^1O_2$ under TP excitation are distinctively different, which are clearly demonstrated in Figure 8e. Here, the increase in the average rate of DCF within the DCFH solution can indirectly reflect the $^1O_2$ generation efficiency of bio-MOF-1&RCs. It is obvious that bio-MOF-1&$[Ru(phen)_3]^{2+}$ and bio-MOF-1&$[Ru(phen)_2hipp]^{2+}$ have considerably high $^1O_2$ yields under TPA. This can be attributed to the existence of an intense electron delocalization conjugate system within the molecular structure of $[Ru(phen)_3]^{2+}$ and $[Ru(phen)_2hipp]^{2+}$; by contrast, such an effect is relatively weak in molecular $[Ru(bpy)_3]^{2+}$. Bio-MOF-1 further extended π-conjugation systems and strengthened the effect within bio-MOF-1&RCs, which resulted in an enhancement of the light harvesting capability in the NIR (near-infrared region) and promoted TP adsorption of bio-MOF-1&$[Ru(phen)_3]^{2+}$ and bio-MOF-1&$[Ru(phen)_2hipp]^{2+}$. In addition, the energy transfer from bio-MOF-1 to RCs in the framework also helped to improve the photocatalytic efficiency of the system for the generation of singlet oxygen.

3. CONCLUSION

In conclusion, we successfully constructed a novel heterogeneous $^1O_2$ generation system using bio-MOF-1&RCs via an ion-exchange process. The bio-MOF-1&RCs exhibited excellent photophysical properties and remarkable emission enhancement. Importantly, bio-MOF-1&RCs have attractive light-harvesting capabilities under NIR through two-photon adsorption. Further, we exploited bio-MOF-1&RCs as photosensitizers for the generation of singlet oxygen in the visible and NIR spectra. Bio-MOF-1&$[Ru(phen)_3]^{2+}$, due to its high electron delocalization conjugate structure, shows extraordinary efficiency for the generation of $^1O_2$ under both SPA and TPA. To the best of our knowledge, this is the first example of using RCs and MOFs to develop a photocatalytic system for the generation of $^1O_2$ by two-photon excitation. These results reveal that bio-MOF-1&RCs are promising candidates as photosensitizers to generate $^1O_2$. We expect that the research of bio-MOF-1&RCs will be further extended in novel application fields such as PDT and chemotherapy integrative collaboration for cancer treatment.

■ ASSOCIATED CONTENT

Supporting Information

The Supporting Information is available free of charge on the ACS Publications website at DOI: 10.1021/acsami.6b05817.

Experimental section and supporting Figures and Tables (PDF)

■ AUTHOR INFORMATION

Corresponding Authors

*E-mail: libinteacher@163.com.
*E-mail: mahp@ciomp.ac.cn.
*E-mail: yuesm458@nenu.edu.cn.

Notes

The authors declare no competing financial interest.

■ ACKNOWLEDGMENTS

The authors gratefully thank the financial support of the NSFC (Grants 51372240, 51572256, and 21501166). This project was supported by the Foundation for Jilin of China of 2014 Human Resources Development.

■ ABBREVIATIONS

RCs, ruthenium(II) complexes; PSs, photosensitizers; bio-MOF-1, $[Zn_8(Ad)_4(BPDC)_6O{\cdot}2Me_2NH_2,\ 8DMF,\ 11H_2O]$; SPA, single-photon absorption; TPA, two-photon absorption; MOFs, metal−organic frameworks; DPBF, 1,3-diphenylisobenzofuran; DCFH, 2,7-dichlorofluorescein; PDT, photodynamic therapy

■ REFERENCES

(1) Ishi-i, T.; Taguri, Y.; Kato, S.-i.; Shigeiwa, M.; Gorohmaru, H.; Maeda, S.; Mataka, S. Singlet Oxygen Generation by Two-Photon Excitation of Porphyrin Derivatives Having Two-Photon-Absorbing Benzothiadiazole Chromophores. *J. Mater. Chem.* **2007**, *17*, 3341−3346.

(2) Schweitzer, C.; Schmidt, R. Physical Mechanisms of Generation and Deactivation of Singlet Oxygen. *Chem. Rev.* **2003**, *103*, 1685−1758.

(3) Liu, J.; Chen, Y.; Li, G.; Zhang, P.; Jin, C.; Zeng, L.; Ji, L.; Chao, H. Ruthenium(II) Polypyridyl Complexes as Mitochondria-Targeted Two-Photon Photodynamic Anticancer Agents. *Biomaterials* **2015**, *56*, 140−153.

(4) Ding, X.; Han, B. H. Metallophthalocyanine-Based Conjugated Microporous Polymers as Highly Efficient Photosensitizers for Singlet Oxygen Generation. *Angew. Chem., Int. Ed.* **2015**, *54*, 6536−6539.

(5) Yao, L.; Dan, F.; Cao, Q.; Mao, M.; Xiao, S. Non-Aggregated Boron-Fluorine Derivatives with Photodynamic Activity. *Appl. Organomet. Chem.* **2012**, *26*, 707−711.

(6) Cakmak, Y.; Kolemen, S.; Duman, S.; Dede, Y.; Dolen, Y.; Kilic, B.; Kostereli, Z.; Yildirim, L. T.; Dogan, A. L.; Guc, D.; Akkaya, E. U. Designing Excited States: Theory-Guided Access to Efficient Photosensitizers for Photodynamic Action. *Angew. Chem., Int. Ed.* **2011**, *50*, 11937−11941.

DOI: 10.1021/acsami.6b05817
ACS Appl. Mater. Interfaces 2016, 8, 21465−21471

(7) Lemercier, G.; Bonne, A.; Four, M.; Lawson-Daku, L. M. ^{3}MLCT Excited States in Ru(II) Complexes: Reactivity and Related Two-Photon Absorption Applications in the near-Infrared Spectral Range. *C. R. Chim.* **2008**, *11*, 709−715.
(8) Yogo, T.; Urano, Y.; Ishitsuka, Y.; Maniwa, F.; Nagano, T. Highly Efficient and Photostable Photosensitizer Based on Bodipy Chromophore. *J. Am. Chem. Soc.* **2005**, *127*, 12162−12163.
(9) Ge, J.; Lan, M.; Zhou, B.; Liu, W.; Guo, L.; Wang, H.; Jia, Q.; Niu, G.; Huang, X.; Zhou, H.; Meng, X.; Wang, P.; Lee, C.-S.; Zhang, W.; Han, X. A graphene quantum dot photodynamic therapy agent with high singlet oxygen generation. *Nat. Commun.* **2014**, *5*, 4596.
(10) Smith, A. M.; Mancini, M. C.; Nie, S. Bioimaging: Second Window for in Vivo Imaging. *Nat. Nanotechnol.* **2009**, *4*, 710−711.
(11) Frederiksen, P. K.; Jørgensen, M.; Ogilby, P. R. Two-Photon Photosensitized Production of Singlet Oxygen. *J. Am. Chem. Soc.* **2001**, *123*, 1215−1221.
(12) Zhang, P.; Huang, H.; Huang, J.; Chen, H.; Wang, J.; Qiu, K.; Zhao, D.; Ji, L.; Chao, H. Noncovalent Ruthenium(II) Complexes-Single-Walled Carbon Nanotube Composites for Bimodal Photothermal and Photodynamic Therapy with near-Infrared Irradiation. *ACS Appl. Mater. Interfaces* **2015**, *7*, 23278−23290.
(13) Zhang, P.; Wang, J.; Huang, H.; Yu, B.; Qiu, K.; Huang, J.; Wang, S.; Jiang, L.; Gasser, G.; Ji, L.; Chao, H. Unexpected high photothemal conversion efficiency of gold nanospheres upon grafting with two-photon luminescent ruthenium(II) complexes: A way towards cancer therapy? *Biomaterials* **2015**, *63*, 102−114.
(14) Zhang, R.; Ye, Z.; Song, B.; Dai, Z.; An, X.; Yuan, J. Development of a Ruthenium(II) Complex-Based Luminescent Probe for Hypochlorous Acid in Living Cells. *Inorg. Chem.* **2013**, *52*, 10325−10331.
(15) Shi, Y.; Liang, M.; Wang, L.; Han, H.; You, L.; Sun, Z.; Xue, S. New Ruthenium Sensitizers Featuring Bulky Ancillary Ligands Combined with a Dual Functioned Coadsorbent for High Efficiency Dye-Sensitized Solar Cells. *ACS Appl. Mater. Interfaces* **2013**, *5*, 144−153.
(16) She, Z.; Cheng, Y.; Zhang, L.; Li, X.; Wu, D.; Guo, Q.; Lan, J.; Wang, R.; You, J. Novel Ruthenium Sensitizers with a Phenothiazine Conjugated Bipyridyl Ligand for High-Efficiency Dye-Sensitized Solar Cells. *ACS Appl. Mater. Interfaces* **2015**, *7*, 27831−27837.
(17) Lv, X.; Wang, F.; Li, Y. Studies of an Extremely High Molar Extinction Coefficient Ruthenium Sensitizer in Dye-Sensitized Solar Cells. *ACS Appl. Mater. Interfaces* **2010**, *2*, 1980−1986.
(18) Fletcher, C.; Keene, F. R.; Anion, F. Interactions with (Polypyridyl)Ruthenium Complexes, and Their Importance in the Cation-Exchange Chromatographic Separation of Stereoisomers of Dinuclear Species [Dagger]. *J. Chem. Soc., Dalton Trans.* **1999**, 683−690.
(19) Spettel, K. E.; Damrauer, N. H. Synthesis, Electrochemical Characterization, and Photophysical Studies of Structurally Tuned Aryl-Substituted Terpyridyl Ruthenium(II) Complexes. *J. Phys. Chem. A* **2014**, *118*, 10649−10662.
(20) Huang, H.; Yu, B.; Zhang, P.; Huang, J.; Chen, Y.; Gasser, G.; Ji, L.; Chao, H. Highly Charged Ruthenium(II) Polypyridyl Complexes as Lysosome-Localized Photosensitizers for Two-Photon Photodynamic Therapy. *Angew. Chem., Int. Ed.* **2015**, *54*, 14049−14052.
(21) Kaspler, P.; Lazic, S.; Forward, S.; Arenas, Y.; Mandel, A.; Lilge, L. A Ruthenium(II) Based Photosensitizer and Transferrin Complexes Enhance Photo-Physical Properties, Cell Uptake, and Photodynamic Therapy Safety and Efficacy. *Photochem. Photobiol. Sci.* **2016**, *15*, 481−495.
(22) Li, S.; Huo, F. Metal-Organic Framework Composites: From Fundamentals to Applications. *Nanoscale* **2015**, *7*, 7482−7501.
(23) Zhu, Q. L.; Xu, Q. Metal-Organic Framework Composites. *Chem. Soc. Rev.* **2014**, *43*, 5468−5512.
(24) Long, J. R.; Yaghi, O. M. The Pervasive Chemistry of Metal-Organic Frameworks. *Chem. Soc. Rev.* **2009**, *38*, 1213−1214.
(25) Murray, L. J.; Dinca, M.; Long, J. R. Hydrogen Storage in Metal-Organic Frameworks. *Chem. Soc. Rev.* **2009**, *38*, 1294−1314.
(26) Li, J.-R.; Kuppler, R. J.; Zhou, H.-C. Selective Gas Adsorption and Separation in Metal-Organic Frameworks. *Chem. Soc. Rev.* **2009**, *38*, 1477−1504.
(27) Li, J.-R.; Sculley, J.; Zhou, H.-C. Metal-Organic Frameworks for Separations. *Chem. Rev.* **2012**, *112*, 869−932.
(28) Kreno, L. E.; Leong, K.; Farha, O. K.; Allendorf, M.; Van Duyne, R. P.; Hupp, J. T. Metal-Organic Framework Materials as Chemical Sensors. *Chem. Rev.* **2012**, *112*, 1105−1125.
(29) Bhattacharjee, S.; Lee, Y.-R.; Puthiaraj, P.; Cho, S.-M.; Ahn, W.-S. Metal-Organic Frameworks for Catalysis. *Catal. Surv. Asia* **2015**, *19*, 203−222.
(30) Zhao, M.; Ou, S.; Wu, C. D. Porous Metal-Organic Frameworks for Heterogeneous Biomimetic Catalysis. *Acc. Chem. Res.* **2014**, *47*, 1199−1207.
(31) Liu, J.; Chen, L.; Cui, H.; Zhang, J.; Zhang, L.; Su, C. Y. Applications of Metal-Organic Frameworks in Heterogeneous Supramolecular Catalysis. *Chem. Soc. Rev.* **2014**, *43*, 6011−6061.
(32) Farrusseng, D.; Aguado, S.; Pinel, C. Metal-Organic Frameworks: Opportunities for Catalysis. *Angew. Chem., Int. Ed.* **2009**, *48*, 7502−7513.
(33) Lee, D. Y.; Lim, I.; Shin, C. Y.; Patil, S. A.; Lee, W.; Shrestha, N. K.; Lee, J. K.; Han, S.-H. Facile Interfacial Charge Transfer across Hole Doped Cobalt-Based MOFs/TiO_2nano-Hybrids Making MOFs Light Harvesting Active Layers in Solar Cells. *J. Mater. Chem. A* **2015**, *3*, 22669−22676.
(34) Jin, S.; Son, H.-J.; Farha, O. K.; Wiederrecht, G. P.; Hupp, J. T. Energy Transfer from Quantum Dots to Metal-Organic Frameworks for Enhanced Light Harvesting. *J. Am. Chem. Soc.* **2013**, *135*, 955−958.
(35) Li, B.; Zhang, Y.; Ma, D.; Ma, T.; Shi, Z.; Ma, S. Metal-Cation-Directed De Novo Assembly of a Functionalized Guest Molecule in the Nanospace of a Metal-Organic Framework. *J. Am. Chem. Soc.* **2014**, *136*, 1202−1205.
(36) So, M. C.; Wiederrecht, G. P.; Mondloch, J. E.; Hupp, J. T.; Farha, O. K. Metal-Organic Framework Materials for Light-Harvesting and Energy Transfer. *Chem. Commun.* **2015**, *51*, 3501−3510.
(37) Lykourinou, V.; Chen, Y.; Wang, X. S.; Meng, L.; Hoang, T.; Ming, L. J.; Musselman, R. L.; Ma, S. Immobilization of MP-11 into a Mesoporous Metal-Organic Framework, MP-11@mesoMOF: A New Platform for Enzymatic Catalysis. *J. Am. Chem. Soc.* **2011**, *133*, 10382−10385.
(38) Park, J.; Feng, D.; Yuan, S.; Zhou, H. C. Photochromic Metal-Organic Frameworks: Reversible Control of Singlet Oxygen Generation. *Angew. Chem., Int. Ed.* **2015**, *54*, 430−435.
(39) Luo, F.; Lin, Y.; Zheng, L.; Lin, X.; Chi, Y. Encapsulation of Hemin in Metal-Organic Frameworks for Catalyzing the Chemiluminescence Reaction of the H_2O_2-Luminol System and Detecting Glucose in the Neutral Condition. *ACS Appl. Mater. Interfaces* **2015**, *7*, 11322−11329.
(40) Evans, J. D.; Sumby, C. J.; Doonan, C. J. Post-Synthetic Metalation of Metal-Organic Frameworks. *Chem. Soc. Rev.* **2014**, *43*, 5933−5951.
(41) Brozek, C. K.; Dinca, M. Cation Exchange at the Secondary Building Units of Metal-Organic Frameworks. *Chem. Soc. Rev.* **2014**, *43*, 5456−5467.
(42) Hergueta-Bravo, A.; Jiménez-Hernández, M. E.; Montero, F.; Oliveros, E.; Orellana, G. Singlet Oxygen-Mediated DNA Photocleavage with Ru(II) Polypyridyl Complexes. *J. Phys. Chem. B* **2002**, *106*, 4010−4017.
(43) Sullivan, B. P.; Salmon, D. J.; Meyer, T. J. Mixed Phosphine 2,2′-Bipyridine Complexes of Ruthenium. *Inorg. Chem.* **1978**, *17*, 3334−3341.
(44) An, J.; Shade, C. M.; Chengelis-Czegan, D. A.; Petoud, S.; Rosi, N. L. Zinc-Adeninate Metal-Organic Framework for Aqueous Encapsulation and Sensitization of near-Infrared and Visible Emitting Lanthanide Cations. *J. Am. Chem. Soc.* **2011**, *133*, 1220−1223.
(45) An, J.; Rosi, N. L. Tuning MOF CO_2 Adsorption Properties Via Cation Exchange. *J. Am. Chem. Soc.* **2010**, *132*, 5578−5579.
(46) Yu, J.; Cui, Y.; Xu, H.; Yang, Y.; Wang, Z.; Chen, B.; Qian, G. Confinement of Pyridinium Hemicyanine Dye within an Anionic

DOI: 10.1021/acsami.6b05817
ACS Appl. Mater. Interfaces 2016, 8, 21465−21471

Metal-Organic Framework for Two-Photon-Pumped Lasing. *Nat. Commun.* **2013**, *4*, 2719.
(47) Chen, Y.; Xu, W.-C.; Kou, J.-F.; Yu, B.-L.; Wei, X.-H.; Chao, H.; Ji, L.-N. Aggregation-Induced Emission of Ruthenium(II) Polypyridyl Complex $[Ru(Bpy)_2(Pzta)]^{2+}$. *Inorg. Chem. Commun.* **2010**, *13*, 1140−1143.
(48) Young, R. H.; Wehrly, K.; Martin, R. L. Solvent effects in dye-sensitized photooxidation reactions. *J. Am. Chem. Soc.* **1971**, *93*, 5774−5779.
(49) Abdel-Shafi, A. A.; Beer, P. D.; Mortimer, R. J.; Wilkinson, F. Photosensitized Generation of Singlet Oxygen from Vinyl Linked Benzo-Crown-Ether-Bipyridyl Ruthenium(II) Complexes. *J. Phys. Chem. A* **2000**, *104*, 192−202.
(50) Sobotta, L.; Fita, P.; Szczolko, W.; Wrotynski, M.; Wierzchowski, M.; Goslinski, T.; Mielcarek, J. Functional singlet oxygen generators based on porphyrazines with peripheral 2,5-dimethylpyrrol-1-yl and dimethylamino groups. *J. Photochem. Photobiol., A* **2013**, *269*, 9−16.
(51) Sour, A.; Jenni, S.; Ortí-Suárez, A.; Schmitt, J.; Heitz, V.; Bolze, F.; Loureiro de Sousa, P.; Po, C.; Bonnet, C. S.; Pallier, A.; Tóth, É.; Ventura, B. Four Gadolinium(III) Complexes Appended to a Porphyrin: A Water-Soluble Molecular Theranostic Agent with Remarkable Relaxivity Suited for MRI Tracking of the Photosensitizer. *Inorg. Chem.* **2016**, *55*, 4545−4554.
(52) Shi, L.; Hernandez, B.; Selke, M. Singlet Oxygen Generation from Water-Soluble Quantum Dot-Organic Dye Nanocomposites. *J. Am. Chem. Soc.* **2006**, *128*, 6278−6279.
(53) Lovell, J. F.; Liu, T. W. B.; Chen, J.; Zheng, G. Activatable Photosensitizers for Imaging and Therapy. *Chem. Rev.* **2010**, *110*, 2839−2857.
(54) Yavin, E.; Weiner, L.; Arad-Yellin, R.; Shanzer, A. Controlling the Energy and Electron Transfer in a Novel Ruthenium Bipyridyl Complex: An Esr Study. *J. Phys. Chem. A* **2001**, *105*, 8018−8024.

DOI: 10.1021/acsami.6b05817
ACS Appl. Mater. Interfaces 2016, 8, 21465−21471